JB Accepted Manuscript Posted Online 26 February 2018
J. Bacteriol. doi:10.1128/JB.00763-17

PhdA catalyzes the first step of phenazine-1-carboxylic acid degradation in *Mycobacterium fortuitum*

Running title: Phenazine-1-carboxylate decarboxylase in *M. fortuitum*

Kyle C Costa[1], Leon S Moskatel[1,*], Lucas A Meirelles[1], and Dianne K Newman[1,2,#]

[1] Division of Biology and Biological Engineering, California Institute of Technology, Pasadena, California, USA, 91125

[2] Division of Geological and Planetary Sciences, California Institute of Technology, Pasadena, California, USA, 91125

[*] Current address: Department of Medicine, Scripps Mercy Hospital, San Diego, CA 92103

[#]Correspondence:
Dianne K Newman
1200 E. California Blvd., Mail code 147-75
Pasadena, CA 91125
Telephone: 626-395-3543
Email: dkn@caltech.edu

ABSTRACT

Phenazines are a class of bacterially-produced redox-active metabolites that are found in natural, industrial, and clinical environments. In *Pseudomonas* spp., phenazine-1-carboxylic acid (PCA)--the precursor of all phenazine metabolites--facilitates nutrient acquisition, biofilm formation, and competition with other organisms. While the removal of phenazines negatively impacts these activities, little is known about the genes or enzymes responsible for phenazine degradation by other organisms. Here, we report that the first step of PCA degradation by *Mycobacterium fortuitum* is catalyzed by a phenazine degrading decarboxylase (PhdA). PhdA is related to members of the UbiD protein family that rely on a prenylated flavin mononucleotide cofactor for activity. PhdB, the enzyme responsible for cofactor synthesis, is present in a putative operon with PhdA in a region of the *M. fortuitum* genome that is essential for PCA degradation. PhdA and PhdB are present in all known PCA degrading organisms from the Actinobacteria. *M. fortuitum* can also catabolize other *Pseudomonas*-derived phenazines such as phenazine-1-carboxamide, 1-hydroxyphenazine, and pyocyanin. Based on our previous work and the current characterization of PhdA, we propose that degradation converges on a common intermediate: dihydroxyphenazine. An understanding of the genes responsible for degradation will enable targeted studies of phenazine degraders in diverse environments.

IMPORTANCE

Bacteria from phylogenetically diverse groups secrete redox active metabolites that provide a fitness advantage for their producers. For example, phenazines from

Pseudomonas spp. benefit producers by facilitating anoxic survival and biofilm formation, and additionally inhibit competitors by serving as antimicrobials. Phenazine-producing pseudomonads act as biocontrol agents by leveraging these antibiotic properties to inhibit plant pests. Despite this importance, the fate of phenazines in the environment is poorly understood. Here we characterize an enzyme from *Mycobacterium fortuitum* that catalyzes the first step of phenazine-1-carboxylic acid degradation. Knowledge of the genetic basis of phenazine degradation will facilitate identification of environments where this activity influences microbial community structure.

INTRODUCTION

Secreted metabolites are common in the microbial world where they play roles in cellular processes such as quorum sensing, signaling, and nutrient acquisition; some additionally act as antimicrobials and inhibit competitors in the environment (1–13). Phenazines are an important class of secreted metabolites named for the three-ringed, heterocyclic phenazine core they share (14). Phenazines are found in clinical, environmental and industrial settings; for example, in agriculture, phenazines produced by *Pseudomonas* spp. are important in biocontrol where they protect dryland cereal crops from a variety of fungal and parasitic infections (15–17). Modification and degradation of phenazines is thought to make plants more susceptible to disease (18). Phenazine-1-carboxylic acid (PCA) is the precursor of all bacterially derived phenazines and is produced by *Pseudomonas* and *Streptomyces* spp.; consequently, PCA has been a target in several efforts to isolate and characterize phenazine degrading organisms (18–20).

To date, all known PCA degrading bacteria belong to either the genus *Sphingomonas* or the suborder Corynebacterineae in the Actinobacteria (18, 20). While all of these organisms can degrade PCA, *Mycobacterium fortuitum* can also degrade the PCA derivatives pyocyanin (PYO), phenazine-1-carboxamide (PCN), 1-hydroxyphenazine (1-OH-PHZ), and phenazine (20, 21). In addition to bacterial degradation, a variety of fungi modify and detoxify phenazines (22, 23). While the capacity to degrade and modify phenazines is well established, and PCA turnover has been documented in situ (19), the genes and proteins catalyzing these activities are poorly characterized.

To understand the role of modification and degradation in situ, a deeper understanding of the genetic basis of these activities is needed. To date, a ~40kb genomic region has been identified in *M. fortuitum* that is essential for the degradation of multiple phenazines (20); contained within this genomic region is a demethylase responsible for the conversion of PYO to 1-OH-PHZ (21). Additionally, multiple dioxygenases are thought to be important for degradation in all known PCA degrading organisms (20, 24–26). Here we expand the known pathways of degradation by characterizing a UbiD-like decarboxylase that catalyzes the conversion of PCA to phenazine. Based on these data and previous genetic experiments, we propose a model for the initial steps in phenazine degradation by *M. fortuitum*.

RESULTS

Phenazine accumulates as an intermediate in PCA degradation by Mycobacterium fortuitum. *M. fortuitum* can completely degrade PCA as a sole source of carbon, energy and nitrogen concomitant with growth (20). Oxygen dependent dioxygenases are important for the complete degradation of PCA; however, when *M. fortuitum* is incubated under anoxic conditions, PCA is still removed from the medium and phenazine begins to accumulate (Figure 1A). These data suggest that phenazine is an intermediate in PCA degradation and that the first step of degradation is catalyzed by a decarboxylase (Figure 1B). In previous work, we identified a ~40kb region of the *M. fortuitum* genome that encodes all known genes for phenazine degradation (20) and others of unknown function (Figure 2). Contained within this region are five annotated decarboxylases that were pursued further.

Heterologous expression and mutagenesis identify the genes necessary for PCA decarboxylation to phenazine. To identify the PCA decarboxylase, each of the five annotated decarboxylases contained within the phenazine responsive region of the *M. fortuitum* strain CT6 genome were expressed in *Escherichia coli* BL21(DE3) (27). After induction, only the strain expressing XA26_16650 (NCBI accession number ALI25512) displayed measurable conversion of PCA to phenazine as assessed by high performance liquid chromatography (HPLC), although with very low activity (Figure 1C). These data suggest that XA26_16650 is the PCA decarboxylase that catalyzes the first step of degradation in *M. fortuitum*. To test this hypothesis, the homolog of XA26_16650 was deleted from the *M. fortuitum* ATCC6841 type strain by replacement with a gentamicin resistance cassette. When incubated on agar plates with 1 mM PCA as the sole carbon source, the mutant was incapable of growth, confirming the necessity of XA26_16650 in PCA degradation (Figure 1D). This growth defect could be complemented by introducing XA26_16650 in trans on the replicative vector pSD5 (28).

PCA degradation is catalyzed by a UbiX/UbiD-like decarboxylase system that is present in all PCA degrading Actinobacteria. XA26_16650 is annotated as a UbiD family decarboxylase. UbiD catalyzes the decarboxylation of 3-polyprenyl-4-hydroxybenzoate to 2-polyprenylphenol in ubiquinone biosynthesis (29). However, ubiquinone is not present in mycobacteria (30) suggesting this gene encodes for another activity. We therefore hypothesize it functions as a PCA decarboxylase, hereafter referred to as phenazine degradation decarboxylase (PhdA). UbiD family decarboxylases utilize a

prenylated flavin mononucleotide (prFMN) cofactor in their active site, which is synthesized by the associated cofactor synthase, UbiX. Consistent with this pattern, there is a UbiX homolog (XA26_16670 (NCBI accession number ALI25514)) oriented directly downstream in an operon with PhdA, hereafter referred to as PhdB (Figure 2) (20).

We have identified several Actinobacteria capable of PCA degradation (20). Among these, three have sequenced genomes (*M. fortuitum*, *Nocardia* sp. LAM0056, and *Rhodococcus* sp. JVH1). In all three cases, a PhdA/PhdB system is present on a region of the genome that is syntenic for gene content (Figure 2). The presence of PhdA/PhdB homologs in each of these organisms, and their absence from close relatives that cannot degrade PCA, further suggests that a core set of genes is important for activity in PCA degrading Actinobacteria.

PhdB is a UbiX-like protein that synthesizes prenylated-FMN. UbiX is a flavin prenyltransferase that synthesizes prFMN from FMN and dimethylallyl monophosphate (DMAP) (31) (Figure 3A). We hypothesized that the *M. fortuitum* UbiX homolog PhdB would catalyze the formation of the prFMN cofactor. An N-terminal 6x-His tag was fused to PhdB and this protein was heterologously expressed in *E. coli* Rosetta(DE3) pLysS. PhdB-His was purified by nickel affinity chromatography (Figure 3B) and assayed for flavin prenyltransferase activity. PhdB-His catalyzed the conversion of reduced FMN to prFMN in the presence of DMAP. The prenylation reaction proceeded to ~90% completion over the course of 3 hours as assayed by liquid chromatography-mass spectrometry (Figure 3C).

PhdA is a UbiD-like protein that catalyzes the decarboxylation of PCA to phenazine. PhdA with a C-terminal 6x-His tag was heterologously expressed in *E. coli* Rosetta(DE3) pLysS and purified by nickel affinity chromatography (Figure 4A). PhdA-His was reconstituted with prFMN under anoxic, reducing conditions. After reconstitution, the bound cofactor was oxidized by exposure to oxygen and incubation at pH 9.2 (32). Interestingly, oxidized PhdA-His lost activity within 2 hours when stored at pH 7, but was stable for several days when stored at pH 9.2.

We found that activity of the oxidized protein was low when incubated with either oxidized or reduced PCA as substrate; however, when supplied with PCA that was premixed with a substoichiometric amount of sodium dithionite, robust activity was observed. PCA, like most phenazines, can exist as a one-electron reduced radical (33), so we hypothesized that a radical may be important to activate the enzyme. At pH 7, phenazines are unstable in their radical form and exist primarily in their oxidized and reduced forms (33); however, paraquat radical is relatively stable at neutral pH (34). Therefore, we hypothesized that paraquat radical would activate the enzyme when supplied in the reaction mixture. This proved to be the case (Figure 4B). Because the prFMN cofactor of UbiD-like proteins is sensitive to over-oxidation (32), we assume that a radical is necessary to achieve the proper oxidation state. More work is necessary to test this or determine if paraquat radical could activate other members of the UbiD family that are poorly active when fully oxidized (32).

PhdA displayed robust activity only when reconstituted with prFMN. PhdA mixed with FMN had little activity and the apoprotein was inactive (Figure 4C). The protein was maximally active at pH 6.9 and in 5% glycerol with no added salt. Under

optimal buffering conditions, the holoenzyme had an apparent K_m of 31.2 ± 6.3 μM and k_{cat} of 82.6 ± 33.5 min^{-1} (mean ± standard deviation, n = 3).

DISCUSSION

We have identified two genes from *M. fortuitum* that are responsible for the decarboxylation of PCA to phenazine, the essential first step in the degradation pathway. PhdA is a member of the UbiD-family of decarboxylases, and PhdB encodes the required prFMN cofactor synthase. At least three genera (*Mycobacterium, Rhodococcus,* and *Nocardia*) in the Actinobacteria contain members capable of PCA degradation based on phenotypic analysis and the presence of PhdA and PhdB homologs in their genomes (Figure 2). Interestingly, while some Proteobacteria can degrade PCA, the pathways they utilize for this activity appear distinct from those in the Actinobacterial phenazine degraders identified to-date. The fact that the genes important for PCA degradation in *M. fortuitum* are also present in other Actinobacterial PCA degrading organisms, and absent from those that lack this activity, further supports the notion that phenazine degradation is catalyzed by a conserved set of genes.

Members of the genus *Sphingomonas* lack *phdA* but still catabolize PCA (18). Biochemical data suggests that this organism may possess a dioxygenase that directly hydroxylates PCA to dihydroxyphenazine (24). However, *in vivo* work suggests that *Sphingomonas* incompletely degrades PCA to 4-hydroxy-1-(2-carboxyphenyl) azacyclobut-2-ene-2-carbonitrile and 4-hydroxy-1-(2-carboxyphenyl)-2-azetidinecarbonitrile (25). These intermediates can only arise when the carboxylate group of PCA is left intact during degradation. Thus, the true pathway of PCA

191 degradation in sphingomonads will require further research to elucidate; it may be that
192 several enzymes in *Sphingomonas* act on PCA. In any case, it is clear that
193 sphingomonads lack homologs of PhdA.

194 While several genera of Actinobacteria are capable of PCA degradation, we have
195 only observed the degradation of additional phenazines like PYO, PCN, and 1-OH-PHZ
196 in *Mycobacterium* spp. (20). We found that an amidase is likely responsible for the
197 conversion of PCN to PCA (20); further decarboxylation of PCA by PhdA yields
198 phenazine as a product. *M. fortuitum* grows with phenazine as a sole source of nitrogen
199 confirming that this compound is readily degraded (20). Several ring hydroxylating
200 dioxygenases are essential for growth with phenazines as a sole carbon source (20); it is
201 likely that one of these acts on phenazine to form phenazine dihydrodiol, which is
202 converted to dihydroxyphenazine through the action of a diol dehydrogenase and further
203 degraded through the action of additional ring-hydroxylating and ring-cleaving
204 dioxygenases. PYO is demethylated by pyocyanin demethylase (PodA) to yield 1-OH-
205 PHZ as a product (21). Genetic evidence suggests that 1-OH-PHZ may be hydroxylated
206 via a monoxygenase activity to yield dihydroxyphenazine (20), but biochemical
207 experiments are necessary to validate this prediction.

208 Thus far, we have not been able to detect intermediates in phenazine degradation
209 by analyzing culture supernatants; however, our genetic and biochemical data lead us to
210 hypothesize that degradation of several phenazines by *Mycobacterium* spp. converge on
211 dihydroxyphenazine as a catabolic intermediate. In previous work, we reported the
212 XA26_16730 dioxygenase to be important for the degradation of PCA because a mutant
213 of this gene could not utilize PCA as a carbon source and accumulated a phenazine in

culture supernatants (20). Therefore, we hypothesize that XA26_16730 (NCBI accession number ALI25520) is the dioxygenase that acts on phenazine to form phenazine dihydrodiol. The putative operon that contains XA26_16730 also encodes a diol dehydrogenase (XA26_16700) that may be responsible for converting phenazine dihydrodiol to dihydroxyphenazine. These observations lead us to propose a model of the degradation pathway where PCN, PCA, PYO and 1-OH-PHZ converge on dihydroxyphenazine as a common intermediate (Figure 5). Future work will test this model of phenazine degradation. The genes identified herein provide a starting point for tracking the presence of phenazine-degrading bacteria in nature, which may facilitate measurements of phenazine turnover in the environment.

METHODS

Strains, medium, and culture conditions. Strains, plasmids, and primers used in this study are listed in Table 1. For routine cultivation, all strains were grown in LB medium (Difco). Where appropriate, either carbenicillin (100 µg ml^{-1}), chloramphenicol (34 µg ml^{-1}), or gentamicin (100 µg ml^{-1}) were included. For medium with PCA as a sole carbon source, *M. fortuitum* was grown in minimal medium with 2 mM PCA (liquid medium) or on plates with 1% noble agar and 1 mM PCA (20). *E. coli* strains were grown at 37 ºC with shaking at 200 rpm and *M. fortuitum* was grown at 30 C with shaking at 200 rpm. PCA was purchased from Princeton Biomolecular Research.

To assess the ability of *E. coli* heterologous expression strains to decarboxylate PCA, *E. coli* BL21 carrying each gene on the replicative vector pET-20b(+) or pET-11a was grown to OD_{600} ~0.5 on LB medium and induced with 200 µM IPTG for 3 hours at

30 ºC. After induction, PCA was added to a final concentration of 100 µM and cells were incubated for an additional 2 hours. Cells were removed by centrifugation and filtered supernatants were analyzed by HPLC. *E. coli* Rosetta expressing His-tagged XA26_16650 and XA26_16670 was grown overnight to stationary phase in LB medium before transfer (1/1000 dilution) to 1 liter of LB medium. Cultures were grown for 5 hours at 37 ºC before induction at 30 ºC with 100 µM IPTG for 3 hours. Cell pellets were collected by centrifugation and stored at -80 C for up to 3 months before protein purification.

Nocardia sp. LAM0056 was isolated by inoculating 3 ml of *Nocardia* PCA medium with 30 mg of soil collected from the California Institute of Technology Campus and incubating at 30°C. *Nocardia* PCA medium contained 17.1 mM NaCl, 1.97 mM $MgCl_2$•$6H_2O$, 0.68 mM $CaCl_2$•$2H_2O$, 6.71 mM KCl, 20 mM phosphate buffer pH 7 (KH_2PO_4/$KHPO_4$), 1 mM $NaSO_4$, 10 mM NH_4Cl, 1 mM PCA, and trace elements and vitamin solutions (35). Cultures were incubated for 1-2 weeks over 3 serial transfers before streak isolation on LB agar medium. DNA was extracted as described previously (20, 36) and sequenced by SMRT sequencing using the Pacific Biosciences RS II platform. De novo genome assembly (37) resulted in 5 contigs. The genome was uploaded to the Integrated Microbial Genomes web server for storage and annotation (https://img.jgi.doe.gov/), IMG genome ID: 2681813501.

Generation of mutants and heterologous expression strains. For heterologous expression, the gene of interest was PCR amplified using primers listed in Table 1, digested with NdeI, NotI, NheI, or BglII (New England Biolabs), and ligated into the

expression vector pET-20b(+) or pET-11a. Plasmids were transformed into either *E. coli* BL21 or Rosetta (Novagen) by electroporation and maintained using antibiotic selection. *M. fortuitum* ATCC6841 ΔMFORT_16229 (ΔXA26_16650, Δ*phdA*) was generated using a recombineering procedure as described previously (28, 38, 39). Briefly, PCR products for the genomic regions flanking MFORT_16229 were ligated to the gentamicin resistance cassette from pMQ30 (40). This linear construct was electroporated into acetamide-induced *M. fortuitum* carrying the plasmid pJV53 (38) as described (39). Mutants were selected on gentamicin-containing medium and screened for the gentamicin cassette at the MFORT_16229 genomic locus by PCR.

To complement the MFORT_16229 deletion, the gene was reintroduced in trans on the replicative vector pSD5 (28). First, the mutant was cured of pJV53 by serial passage (20). The coding sequence of MFORT_16229 was ligated into the NdeI and PstI (enzymes from New England Biolabs) sites of pSD5, and the resulting construct was electroporated into *M. fortuitum* ΔMFORT_16229. Cultures containing the plasmid were selected on containing kanamycin (100 μg ml^{-1}).

HPLC analysis of small molecules. HPLC analysis was performed on a Waters Alliance e2695 equipped with a 2998 photodiode array detector and a Acquity QDa mass spectrometry detector. To track PCA and phenazine, a gradient of water with 0.1% NH_4OH (buffer A) to 80% acetonitrile with 0.1% NH_4OH (buffer B) was run on an XBridge C18 3.5 μm (2.1 x 50 mm) column. QDa was run with a cone voltage of 5 V and a capillary voltage of 0.8 kV and analytes were measured at 367 nm wavelength. Samples were run at a flow rate of 0.3 ml min^{-1} with a linear gradient of from 0 – 100%

283 buffer B for 10 minutes, 2 minutes at 100% buffer B, and a reequilibration for 6 minutes
284 at 0% buffer B. To determine kinetic parameters for PhdA, samples were loaded on a
285 Beckman System Gold HPLC equipped with a photo diode array detector and a XBridge
286 phenyl 5 µm (4.6 x 250 mm) column; data was collected at 250 nm. Samples were run at
287 a flow rate of 0.95 ml min^{-1} and purified with a gradient of water with 0.1% NH_4OH
288 (buffer A) to 100% acetonitrile with 0.1% NH_4OH (buffer C) using the following
289 method: a linear gradient from 0% to 50% buffer C for 1 minute, a linear gradient of 50%
290 to 90% buffer C for 11 minutes, 90% to 0% buffer C for 1 minute, and a reequilibration
291 for 5 minutes at 0% buffer C.
292
293 ***Purification of the PhdA and PhdB.*** Cell pellets of *E. coli* strains were lysed by
294 sonication using a Fisher Scientific 550 sonic dismembrator set to four with five second
295 pulses at 25 second intervals. Particulate debris was removed by centrifugation at 50,000
296 xg for 20 minutes and supernatants were applied to a HisTrap HP 5 ml nickel column on
297 an ÄKTApurifier FPLC (GE healthcare). Proteins were eluted in buffers containing 500
298 mM NaCl, 5% glycerol, 20 mM Tris (pH 7.2) over a gradient from 20 mM to 500 mM
299 imidazole applied over 10 column volumes. Proteins were concentrated by centrifugation
300 (Amicon Ultra-15 centrifugal filters, Ultracel 10K MWCO) as necessary. Proteins were
301 used the same day as they were purified for subsequent analysis.
302
303 ***Synthesis of prenylated-FMN.*** Prenylated-FMN was synthesized using purified
304 XA26_16670-His (PhdB-His), reduced FMN, and dimethyl-allyl monophosphate
305 (DMAP). DMAP was synthesized from 3-methyl-2-buten-1-ol and tetrabutylammonium

306 phosphate (Sigma) as described (41). Fractions with DMAP were identified by thin layer
307 chromatography and molybdate reagent. Trace tetrabutylammonium phosphate
308 contaminant was removed by ion exchange across Amberlite IR120 resin, hydrogen form
309 that was pre-washed with 75% ammonium hydroxide, equilibrated with 100 mM
310 ammonium bicarbonate, and eluted with 100 mM ammonium bicarbonate. DMAP was
311 recovered by lyophilization as a white powder. Purified PhdB-His was mixed with 2.5
312 mM reduced FMN (reduced with a 4-fold molar excess of sodium dithionite) and a 2-fold
313 molar excess of DMAP under anaerobic conditions (Coy glovebox with a 5% H_2/95% N_2
314 atmosphere) in a buffer consisting of 500 mM NaCl, 5% glycerol, Tris pH 7 (32). The
315 reaction mixture was left to incubate for 3 hours and monitored by HPLC until at least
316 90% of the FMN was converted to prFMN. The synthesized prFMN product was
317 separated from PhdB-His by filtration through a 10k MWCO membrane (Microcon
318 Ultracel YM-10 regenerated cellulose) and assumed to be present at a 2.5 mM
319 concentration in subsequent experiments.
320
321 ***Decarboxylation of PCA by PhdA.*** PhdA was reconstituted with prFMN under anoxic
322 conditions in a buffer containing 500 mM NaCl, 5% glycerol, Tris pH7.2, 1 mM reduced
323 prFMN, 4 mM $MnCl_2$ and 4 mM KCl (32). After a 10-minute incubation, protein was
324 oxidized by exposure to atmospheric oxygen and buffer exchanged to pH 9.2. Complete
325 oxidation (assessed by visual color change from purple to yellow) occurred after ~3 hours
326 at pH 9.2 (32). To generate paraquat radical, 10 mM paraquat was mixed with 5 mM
327 sodium dithionite under anoxic conditions. A substoichiometric amount of sodium
328 dithionite was used to avoid reduction of prFMN in subsequent steps. Reconstituted,

oxidized PhdA was brought into a Coy anaerobic chamber and added directly (50 – 100 nM final concentration) to buffer containing 5% glycerol, Bis-Tris pH 6.9, and 100 µM paraquat radical and incubated for 10 minutes before the addition of varying concentrations of PCA (2-500 µM). Substrates were mixed with PhdA for 5 minutes before the reaction was quenched by the addition of NH_4OH (10% final volume). Apparent kinetic parameters for PhdA were determined by monitoring the appearance of phenazine by HPLC. Kinetic parameters were calculated in excel as previously described (42).

ACKNOWLEDGEMENTS

We thank members of the Newman lab for experimental advice and feedback on the manuscript. Grants to D.K.N. from the ARO (W911NF-17-1-0024) and NIH (1R01AI127850-01A1) supported this research. K.C.C. was supported by a Ruth L. Kirschstein National Research Service Award from the NIH, National Institute of Allergy and Infectious Diseases, Grant no. F32AI112248.

REFERENCES

1. **Raymond KN**, **Müller G**, **Matzanke BF**. 1984. Complexation of iron by siderophores a review of their solution and structural chemistry and biological function. Top Curr Chem **123**:49-102.
2. **Hernandez ME**, **Newman DK**. 2001. Extracellular electron transfer. Cell Mol Life Sci **58**:1562–1571.
3. **Waters CM**, **Bassler BL**. 2005. Quorum sensing: cell-to-cell communication in bacteria. Annu Rev Cell Dev Biol **21**:319–346.
4. **Davies J**. 2007. Small molecules: the lexicon of biodiversity. J Biotechnol **129**:3–5.
5. **Davies J**, **Ryan KS**. 2012. Introducing the parvome: bioactive compounds in the microbial world. ACS Chem Biol **7**:252–259.
6. **Schuster M**, **Sexton DJ**, **Diggle SP**, **Greenberg EP**. 2013. Acyl-homoserine lactone quorum sensing: from evolution to application. Annu Rev Microbiol **67**:43–63.
7. **Traxler MF**, **Kolter R**. 2015. Natural products in soil microbe interactions and evolution. Nat Prod Rep **32**:956–970.
8. **Abreu NA**, **Taga ME**. 2016. Decoding molecular interactions in microbial communities. FEMS Microbiol Rev **40**:648–663.
9. **Fischbach MA**, **Segre JA**. 2016. Signaling in host-associated microbial communities. Cell **164**:1288–1300.
10. **Papenfort K**, **Bassler BL**. 2016. Quorum sensing signal-response systems in Gram-negative bacteria. Nat Rev Microbiol **14**:576–588.
11. **Springer SD**, **Butler A**. 2016. Microbial ligand coordination: Consideration of

biological significance. Coord Chem Rev **306**:628–635.

12. **Glasser NR**, **Saunders SH**, **Newman DK**. 2017. The colorful world of extracellular electron shuttles. Annu Rev Microbiol **71**:731–751.

13. **Whiteley M**, **Diggle SP**, **Greenberg EP**. 2017. Progress in and promise of bacterial quorum sensing research. Nature **551**:313–320.

14. **Price-Whelan A**, **Dietrich LEP**, **Newman DK**. 2006. Rethinking "secondary" metabolism: physiological roles for phenazine antibiotics. Nat Chem Biol **2**:71–78.

15. **Huang Z**, **Bonsall RF**, **Mavrodi DV**, **Weller DM**, **Thomashow LS**. 2004. Transformation of *Pseudomonas fluorescens* with genes for biosynthesis of phenazine-1-carboxylic acid improves biocontrol of rhizoctonia root rot and in situ antibiotic production. FEMS Microbiol Ecol **49**:243–251.

16. **Yang M-M**, **Mavrodi DV**, **Mavrodi OV**, **Bonsall RF**, **Parejko JA**, **Paulitz TC**, **Thomashow LS**, **Yang H-T**, **Weller DM**, **Guo J-H**. 2011. Biological control of take-all by fluorescent *Pseudomonas* spp. from Chinese wheat fields. Phytopathology **101**:1481–1491.

17. **Mavrodi DV**, **Mavrodi OV**, **Parejko JA**, **Bonsall RF**, **Kwak Y-S**, **Paulitz TC**, **Thomashow LS**, **Weller DM**. 2012. Accumulation of the antibiotic phenazine-1-carboxylic acid in the rhizosphere of dryland cereals. Appl Environ Microbiol **78**:804–812.

18. **Yang Z-J**, **Wang W**, **Jin Y**, **Hu H-B**, **Zhang X-H**, **Xu Y-Q**. 2007. Isolation, identification, and degradation characteristics of phenazine-1-carboxylic acid-degrading strain *Sphingomonas* sp. DP58. Curr Microbiol **55**:284–287.

19. **Mavrodi DV**, **Parejko JA**, **Mavrodi OV**, **Kwak Y-S**, **Weller DM**, **Blankenfeldt**

W, **Thomashow LS**. 2013. Recent insights into the diversity, frequency and ecological roles of phenazines in fluorescent *Pseudomonas* spp. Environ Microbiol **15**:675–686.

20. **Costa KC**, **Bergkessel M**, **Saunders S**, **Korlach J**, **Newman DK**. 2015. Enzymatic degradation of phenazines can generate energy and protect sensitive organisms from toxicity. mBio **6**:e01520-15.

21. **Costa KC**, **Glasser NR**, **Conway SJ**, **Newman DK**. 2017. Pyocyanin degradation by a tautomerizing demethylase inhibits *Pseudomonas aeruginosa* biofilms. Science **355**:170–173.

22. **Hill JC**, **Johnson GT**. 1969. Microbial transformation of phenazines by *Aspergillus sclerotiorum*. Mycologia **61**:452–467.

23. **Moree WJ**, **Phelan VV**, **Wu C-H**, **Bandeira N**, **Cornett DS**, **Duggan BM**, **Dorrestein PC**. 2012. Interkingdom metabolic transformations captured by microbial imaging mass spectrometry. Proc Natl Acad Sci U S A **109**:13811–13816.

24. **Zhao Q**, **Hu H-B**, **Wang W**, **Huang X-Q**, **Zhang X-H**. 2017. Identification and characterization of a novel three-component phenazine-1-carboxylic acid 1, 2-dioxygenase in *Sphingomonas wittichii* DP58. Appl Environ Microbiol **83**:e00133-17.

25. **Chen K**, **Hu H**, **Wang W**, **Zhang X**, **Xu Y**. 2008. Metabolic degradation of phenazine-1-carboxylic acid by the strain *Sphingomonas* sp. DP58: the identification of two metabolites. Biodegradation **19**:659–667.

26. **Ma Z**, **Shen X**, **Hu H**, **Wang W**, **Peng H**, **Xu P**, **Zhang X**. 2012. Genome

sequence of *Sphingomonas wittichii* DP58, the first reported phenazine-1-carboxylic acid-degrading strain. J Bacteriol **194**:3535–3536.

27. **Studier FW**, **Moffatt BA**. 1986. Use of bacteriophage T7 RNA polymerase to direct selective high-level expression of cloned genes. J Mol Biol **189**:113–130.

28. **DasGupta SK**, **Jain S**, **Kaushal D**, **Tyagi AK**. 1998. Expression systems for study of mycobacterial gene regulation and development of recombinant BCG vaccines. Biochem Biophys Res Commun **246**:797–804.

29. **Jacewicz A**, **Izumi A**, **Brunner K**, **Schnell R**, **Schneider G**. 2013. Structural insights into the UbiD protein family from the crystal structure of PA0254 from *Pseudomonas aeruginosa*. PLoS ONE **8**:e63161.

30. **Schoepp-Cothenet B**, **van Lis R**, **Atteia A**, **Baymann F**, **Capowiez L**, **Ducluzeau A-L**, **Duval S**, **ten Brink F**, **Russell MJ**, **Nitschke W**. 2013. On the universal core of bioenergetics. Biochim Biophys Acta **1827**:79–93.

31. **White MD**, **Payne KAP**, **Fisher K**, **Marshall SA**, **Parker D**, **Rattray NJW**, **Trivedi DK**, **Goodacre R**, **Rigby SEJ**, **Scrutton NS**, **Hay S**, **Leys D**. 2015. UbiX is a flavin prenyltransferase required for bacterial ubiquinone biosynthesis. Nature **522**:502–506.

32. **Marshall SA**, **Fisher K**, **Ni Cheallaigh A**, **White MD**, **Payne KAP**, **Parker DA**, **Rigby SEJ**, **Leys D**. 2017. Oxidative maturation and structural characterization of prenylated-FMN binding by UbiD, a decarboxylase involved in bacterial ubiquinone biosynthesis. J Biol Chem **292**:4623-4637.

33. **Friedheim E**, **Michaelis L**. 1931. Potentiometric study of pyocyanine. J Biol Chem **91**:355-368.

34. **Bockman TM**, **Kochi JK**. 1990. Isolation and oxidation-reduction of methylviologen cation radicals. Novel disproportionation in charge-transfer salts by X-ray crystallography. J Org Chem **55**:4127–4135.

35. **Whitman WB**, **Shieh J**, **Sohn S**, **Caras… DS**. 1986. Isolation and characterization of 22 mesophilic methanococci. Syst Appl Microbiol **7**: 35-240.

36. **Belisle JT**, **Mahaffey SB**, **Hill PJ**. 2009. Isolation of mycobacterium species genomic DNA. Methods Mol Biol **465**:1–12.

37. **Chin C-S**, **Alexander DH**, **Marks P**, **Klammer AA**, **Drake J**, **Heiner C**, **Clum A**, **Copeland A**, **Huddleston J**, **Eichler EE**, **Turner SW**, **Korlach J**. 2013. Nonhybrid, finished microbial genome assemblies from long-read SMRT sequencing data. Nat Methods **10**:563–569.

38. **van Kessel JC**, **Hatfull GF**. 2007. Recombineering in *Mycobacterium tuberculosis*. Nat Methods **4**:147–152.

39. **Goude R**, **Roberts DM**, **Parish T**. 2015. Electroporation of mycobacteria. Methods Mol Biol **1285**:117–130.

40. **Shanks RMQ**, **Caiazza NC**, **Hinsa SM**, **Toutain CM**, **O'Toole GA**. 2006. *Saccharomyces cerevisiae*-based molecular tool kit for manipulation of genes from gram-negative bacteria. Appl Environ Microbiol **72**:5027–5036.

41. **Lira LM**, **Vasilev D**, **Pilli RA**, **Wessjohann LA**. 2013. One-pot synthesis of organophosphate monoesters from alcohols. Tetrahedron Letters **54**:1690–1692.

42. **Kemmer G**, **Keller S**. 2010. Nonlinear least-squares data fitting in Excel spreadsheets. Nat Protoc **5**:267–281.

459 **FIGURE LEGENDS**

460 **Figure 1** – ***Mycobacterium fortuitum*** **catalyzes PCA decarboxylation as the first step**
461 **in degradation. A.** Cultures of *M. fortuitum* incubated under anoxic conditions and in
462 the presence of PCA catalyzed the formation of phenazine. PCA elutes around the four-
463 minute mark and phenazine elutes around the eight minute mark. **B.** The proposed
464 reaction catalyzed by *M. fortuitum*. **C.** *E. coli* strains expressing individual
465 decarboxylase genes. Phenazine accumulation was only observed in the presence of the
466 *M. fortuitum* gene XA26_16650. **D.** *M. fortuitum* lacking the gene XA26_16650 cannot
467 grow on medium with PCA provided as the sole carbon source. When the mutation is
468 complemented in trans (+pSD5-16650), growth is restored.

469

470 **Figure 2** – **A genomic region responsible for PCA degradation is conserved in**
471 **different species.** The genomic region contains genes encoding dioxygenases (grey),
472 decarboxylases (black), and a pyocyanin demethylase (PodA, striped). Most of the genes
473 from *M. fortuitum*, including PhdA, are conserved in the PCA degraders *Rhodococcus* sp.
474 JVH1 and *Nocardia* sp. LAM0056. Genes that are conserved across genomes are
475 indicated with grey shading.

476

477 **Figure 3** – **PhdB (XA26_16670) is a flavin prenyltransferase that synthesizes**
478 **prFMN. A**. The reaction catalyzed by PhdB. **B**. SDS-PAGE gel showing purified PhdB
479 protein. **C**. LC-MS of the reaction catalyzed by PhdB. FMN starting material is
480 converted to prFMN over the course of 3 hours in the presence of DMAP and PhdB. The
481 reaction proceeded to ~90% completion as assessed by the loss of FMN.

Figure 4 – **The reaction catalyzed by PhdA. A**. SDS-PAGE gel showing purified PhdA protein. **B**. PhdA is only active when incubated with paraquat radical. Protein was incubated for 10 minutes with paraquat radical at concentrations ranging from 50 nM to 0.5 mM before the addition of 1 mM PCA and displayed a dose dependent response in activity. **C**. PhdA catalyzes the conversion of PCA to phenazine only when reconstituted with the prFMN cofactor. FMN cannot act as a cofactor for the protein.

Figure 5 – **Proposed pathway for the first steps in phenazine degradation by *M. fortuitum*.** PYO, 1-OH-PHZ, PCN, and PCA converge on dihydroxyphenazine as a common intermediate. Dihydroxyphenazine is likely further degraded through the action of multiple ring-cleaving and ring-hydroxylating dioxygenases.

Strains

name	description
M. fortuitum strain CT6	wild-type *M. fortuitum*, DNA used for heterologous expression
M. fortuitum ATCC6841	wild-type *M. fortuitum*, type strain
M. fortuitum Δ*phdA*	ATCC6841 with an in-frame deletion of *phdA* (XA26_16650)
M. fortuitum Δ*phdA*, pSD5-*phdA*	ATCC6841 with an in-frame deletion of *phdA* (XA26_16650) and *phdA* complemented in trans
Nocardia sp. LAM0056	wild-type
E. coli Rosetta pET-20b(+)-*phdA-His*	Expression construct to generate PhdA-His protein
E. coli Rosetta pET-20b(+)-*phdB-His*	Expression construct to generate PhdB-His protein
E. coli BL21(DE3) pET-20b(+)-16650	Expression construct
E. coli BL21(DE3) pET-20b(+)-16670	Expression construct
E. coli BL21(DE3) pET-20b(+)-16790	Expression construct
E. coli BL21(DE3) pET-11a-16920	Expression construct
E. coli BL21(DE3) pET-20b(+)-16950	Expression construct

Primers

name	notes	sequence
16650-NdeI-F	expression	AAAACATATGGCGGTTTTCCGTGACTTGCGGCATTACATCGACA
16650-NotI-R	expression	TTTTGCGGCCGCTCAGAGCGGCAATGTCGCCTTCCACCGATCGCGGA
16670-NdeI-F	expression	AAAACATATGCGCATCATCGTCGCGATCAGCGGCGCCA
16670-NotI-R	expression	TTTTGCGGCCGCCTACTCGGTGCCGGCAGCTTGA
16790-NdeI-F	expression	AAAACATATGAACATCGAATTCAGCACCGTAATCCAGCCCA
16790-NotI-R	expression	TTTTGCGGCCGCTCAGCAGGCCAGGGTGACGGACCTCAGCGA
16920-NheI-F	expression	AAAAATGGCTAGCCCTGAACACAGTTCACCGATCGCAAGGGCGTTACT
16920-BglII-R	expression	TTTTAGATCTTCATCCTTCTCCGTCAGCAGCGAAACAT
16950-NdeI-F	expression	AAAACATATGACCAGCGCAACGCAGTGGAGTGTCTCGA
16950-NotI-R	expression	TTTTGCGGCCGCCTACTCCGCGCCGAGCGCGACGGTGCCGAGGT
16650His-NotI-R	expression	AAAAGCGGCCGCTCAATGGTGATGGTGATGGTGGCTCTGGAAGTACAGGT TTTCGGCGAGCGGCAATGTCGCCTTCCACCGATCGCGGA
16670-His-NotI-R	expression	TTTTGCGGCCGCTCAATGGTGATGGTGATGGTGGCTCTGGAAGTACAGGTT TTCGGCCTCGGTGCCGGCAGCTTGACTGAGGTCAT
phdA-us-F	Δ*phdA*	CGTTTACGTAGTCTGGCGACCGCCCGAGCAGT
phdA -us-R-XbaI	Δ*phdA*	TTTTTCTAGAATGTCCAATAGATGGTTCGGATATCCATCATCCGATTCACA
phdA -ds-F-NotI	Δ*phdA*	AAAAGCGGCCGCCGGGGTCGAGGAAGGTGGAAAGTGATGACGT
phdA -ds-R	Δ*phdA*	CGTATCACGCATCACGGCTGCTCGTATCCCGCGCGGAGT
phdA-F-NdeI	complementation	AAAACATATGGGGGGCTCGGCGCGCAAGGTGGAAGTGCAGAGCCA
phdA-R-PstI	complementation	TTTTCTGCAGTCAGAGCGGCAATGTCGCCTTCCACCGATCGCGGATCT

Table 1. Strains and primers used in this study

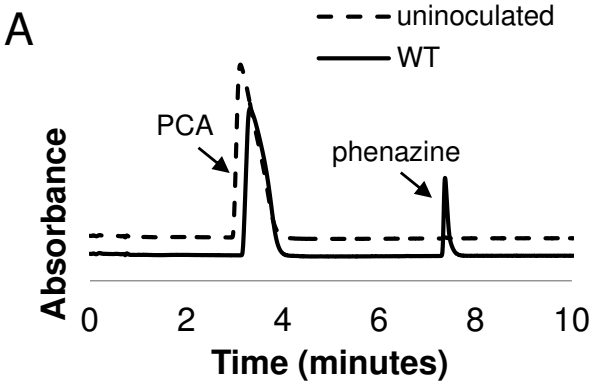

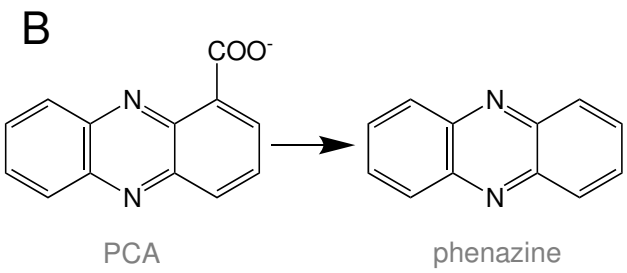

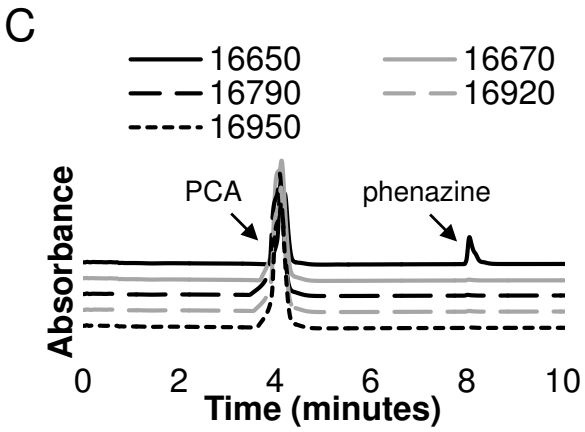

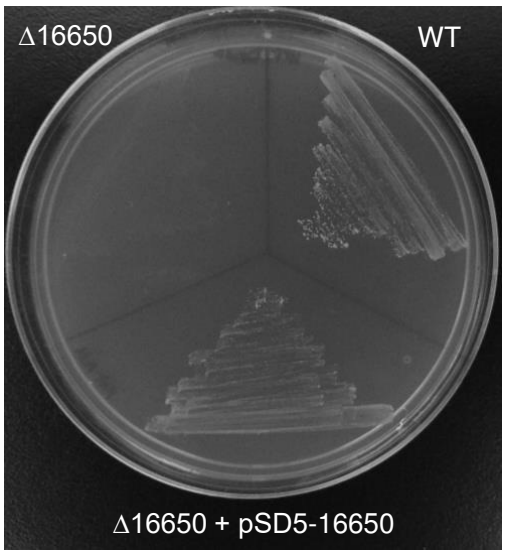

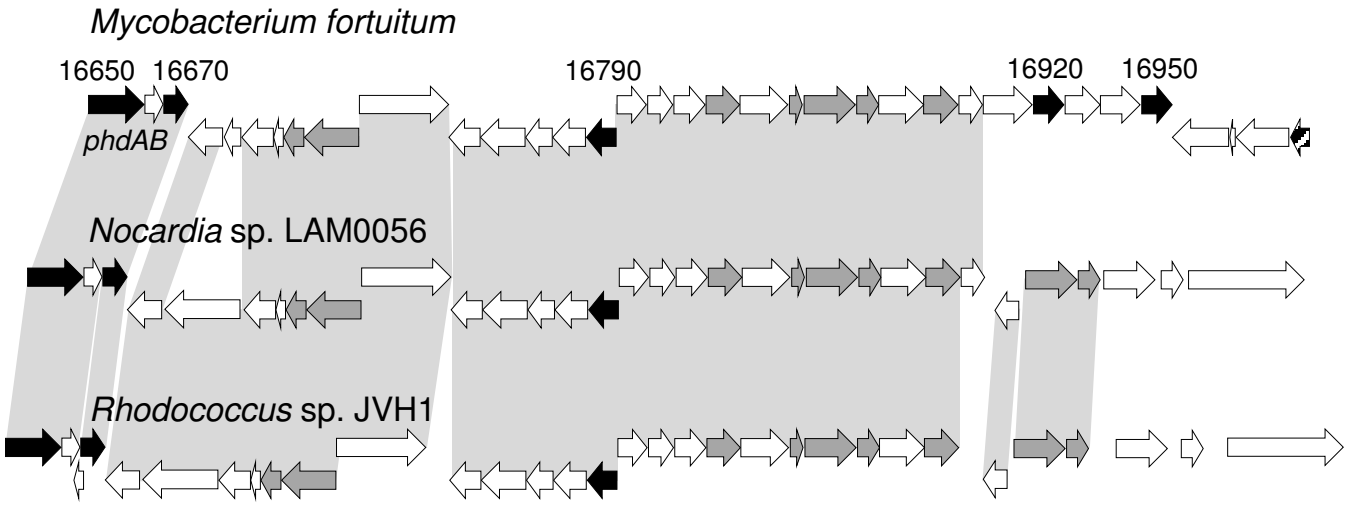

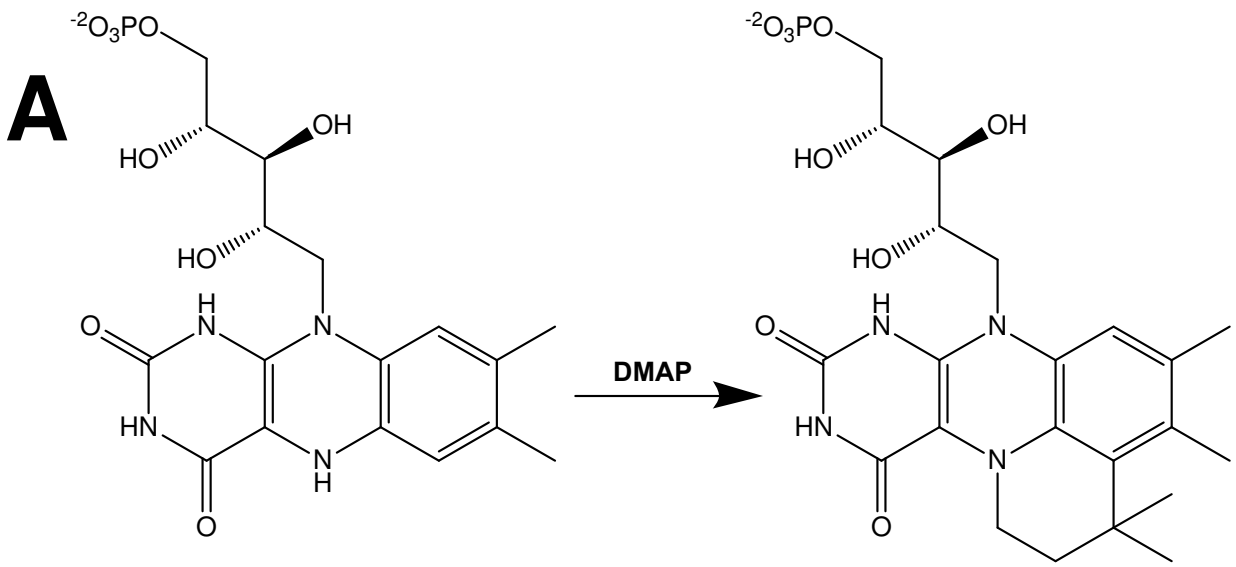

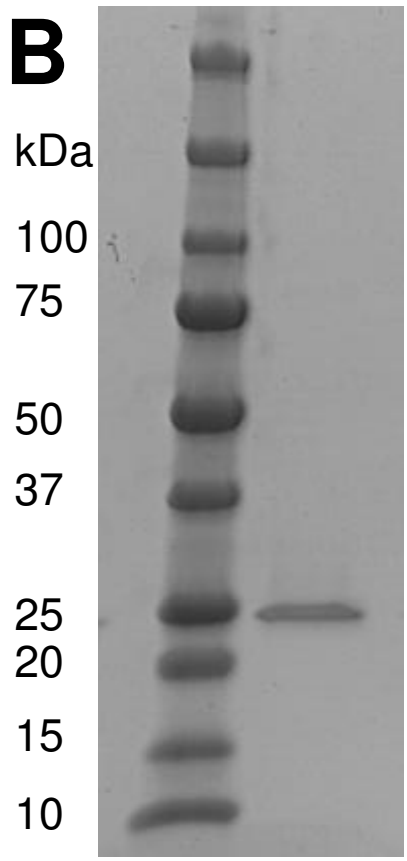

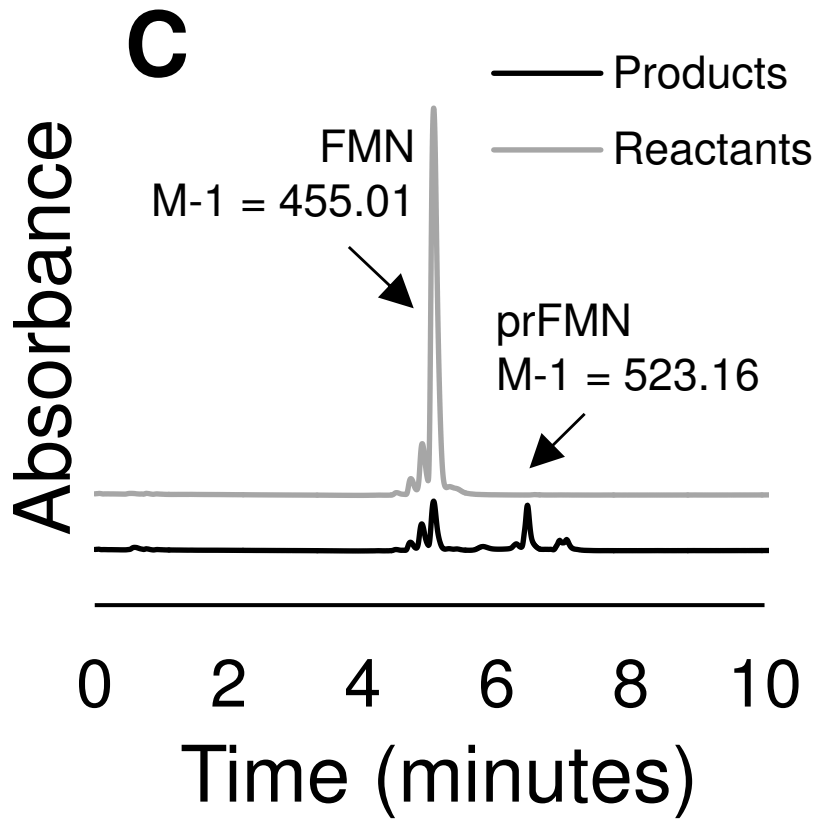

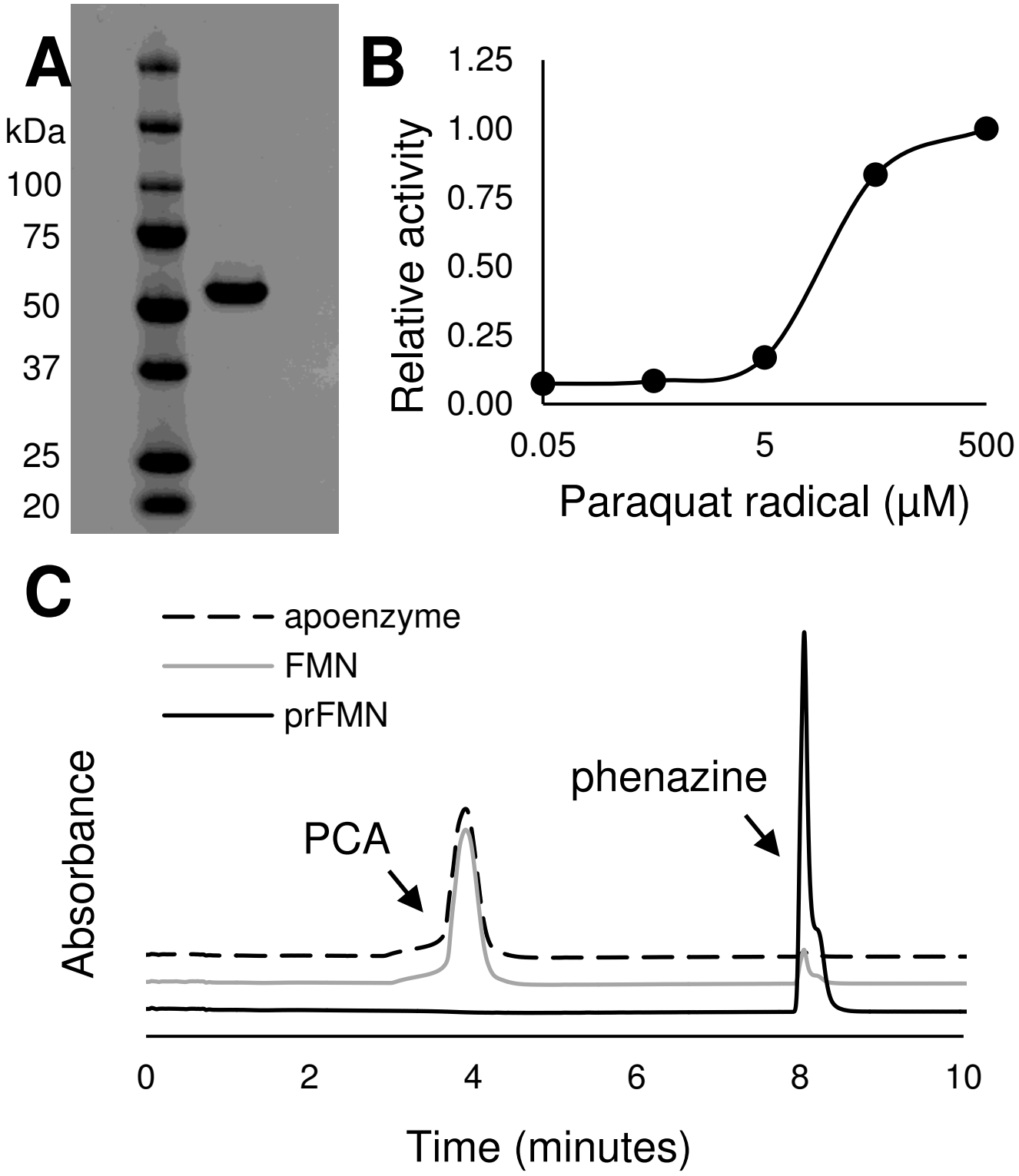

Journal of Bacteriology
JB
Journal of Bacteriology